


RESEARCH ARTICLE

Open Access



Amino acid mutations PB1-V719M and PA-N444D combined with PB2-627K contribute to the pathogenicity of H7N9 in mice

Xiaoquan Wang^{1,2,3,4†}, Xin-en Tang^{1†}, Huafen Zheng¹, Ruyi Gao^{1,3,4}, Xiaolong Lu^{1,3,4}, Wenhao Yang^{1,3,4}, Le Zhou⁵, Yu Chen^{1,3,4}, Min Gu^{1,3,4}, Jiao Hu^{1,3,4}, Xiaowen Liu^{1,3,4}, Shunlin Hu^{1,3,4}, Kaituo Liu^{1,2,3,4*}  and Xiufan Liu^{1,2,3,4*}

Abstract

H7N9 subtype avian influenza viruses (AIVs) cause 1567 human infections and have high mortality, posing a significant threat to public health. Previously, we reported that two avian-derived H7N9 isolates (A/chicken/Eastern China/JTC4/2013 and A/chicken/Eastern China/JTC11/2013) exhibit different pathogenicities in mice. To understand the genetic basis for the differences in virulence, we constructed a series of mutant viruses based on reverse genetics. We found that the PB2-E627K mutation alone was not sufficient to increase the virulence of H7N9 in mice, despite its ability to enhance polymerase activity in mammalian cells. However, combinations with PB1-V719M and/or PA-N444D mutations significantly enhanced H7N9 virulence. Additionally, these combined mutations augmented polymerase activity, thereby intensifying virus replication, inflammatory cytokine expression, and lung injury, ultimately increasing pathogenicity in mice. Overall, this study revealed that virulence in H7N9 is a polygenic trait and identified novel virulence-related residues (PB2-627K combined with PB1-719M and/or PA-444D) in viral ribonucleoprotein (vRNP) complexes. These findings provide new insights into the molecular mechanisms underlying AIV pathogenesis in mammals, with implications for pandemic preparedness and intervention strategies.

Keywords H7N9, pathogenicity, virulence factors, vRNP

Introduction

As members of the Orthomyxoviridae family of viruses, influenza A viruses (IAVs) have eight-segmented, negative, single-stranded RNA genomes. In accordance with the antigenic specificity of hemagglutinin (HA) and neuraminidase (NA) proteins on the surface of IAVs, they can be categorized into subtypes H1–H18 and N1–N11, respectively. Except for subtypes H17N10 and H18N11, which are exclusively found in bats [1, 2], all other HA and NA subtype strains primarily originate from wild birds and poultry and are collectively referred to as avian influenza viruses (AIVs) [3]. During more than a century of evolution since the first report of AIVs in Italy in 1878, AIVs have gradually been able to cross interspecies barriers, infecting a wide range of mammals, including humans [3–5].

Handling editor: Marie Galloux.

[†]Xiaoquan Wang and Xin-en Tang contributed equally to the work.

*Correspondence:

Kaituo Liu

liukaituo@yzu.edu.cn

Xiufan Liu

xfliu@yzu.edu.cn

¹ College of Veterinary Medicine, Yangzhou University, Yangzhou 225009, China

² Joint International Research Laboratory of Agriculture and Agri-Product Safety, The Ministry of Education of China, Yangzhou University, Yangzhou 225009, China

³ Jiangsu Co-innovation Center for Prevention and Control of Important Animal Infectious Diseases and Zoonosis, Yangzhou University, Yangzhou 225009, China

⁴ Jiangsu Key Laboratory of Zoonosis, Yangzhou 225009, China

⁵ Yangzhou Center for Disease Control and Prevention, Yangzhou 225009, China



© The Author(s) 2024. **Open Access** This article is licensed under a Creative Commons Attribution 4.0 International License, which permits use, sharing, adaptation, distribution and reproduction in any medium or format, as long as you give appropriate credit to the original author(s) and the source, provide a link to the Creative Commons licence, and indicate if changes were made. The images or other third party material in this article are included in the article's Creative Commons licence, unless indicated otherwise in a credit line to the material. If material is not included in the article's Creative Commons licence and your intended use is not permitted by statutory regulation or exceeds the permitted use, you will need to obtain permission directly from the copyright holder. To view a copy of this licence, visit <http://creativecommons.org/licenses/by/4.0/>. The Creative Commons Public Domain Dedication waiver (<http://creativecommons.org/publicdomain/zero/1.0/>) applies to the data made available in this article, unless otherwise stated in a credit line to the data.

Multiple subtypes of AIV can infect humans, including H5N1/6, H7N4/9, H10N3/8, H3N8 and H9N2 [6–13]. Among them, H7N9 subtype AIVs cause the greatest number of human infections (1568 cases) and are associated with a high fatality rate (39%), posing a serious threat to public health [14]. In this regard, exploring the mechanisms that enhance the infectivity and pathogenicity of H7N9 in mammals is important.

AIVs typically exhibit low pathogenicity in mice, although certain strains can unexpectedly become highly pathogenic without the need for prior adaptation [15]. As we reported previously, two avian-derived H7N9 isolates, namely, A/chicken/Eastern China/JTC4/2013 (JTC4) and A/chicken/Eastern China/JTC11/2013 (JTC11), are genetically highly similar but exhibit different pathogenicities in mice [16]. The five proteins encoded by the JTC4 and JTC11 viruses differ by only six amino acids located in five different proteins, i.e., polymerase basic protein 2 (PB2), PB1, polymerase acid protein (PA), HA and NA. To understand the genetic basis for the different virulence levels of the two H7N9 viruses in mice, we generated a series of mutation viruses using reverse genetics. Our study revealed that the synergy among polymerase proteins is the pivotal molecular mechanism influencing the virulence of H7N9 in mice.

Materials and methods

Viruses and cell lines

The H7N9-subtype AIVs A/Chicken/Eastern China/JTC4/2013 and A/Chicken/Eastern China/JTC11/2013 were obtained from chickens and preserved in our laboratory [16]. The viruses were amplified in 9-day-old specific-pathogen-free (SPF) embryonated eggs (Merial, China) and stored at -80°C . Primary chicken embryo fibroblasts (CEFs) were prepared in our laboratory. Human embryonic kidney 293 (HEK293T), Madin-Darby canine kidney (MDCK), and human lung carcinoma (A549) cells were grown in Dulbecco's modified Eagle's medium (DMEM; Invitrogen, USA) supplemented with 10% fetal bovine serum (FBS; Gibco, New Zealand).

Plasmid construction and viral rescue

All gene segments of A/Chicken/Eastern China/JTC4/2013 and A/Chicken/Eastern China/JTC11/2013 were cloned and inserted into the pHW2000 vector, as previously described [17]. Eight plasmids were co-transfected into HEK293T cells using Lipofectamine 2000 Reagent (Invitrogen, USA). Culture supernatant aliquots were harvested at 72 h post-transfection, and 9-day-old chicken embryos were infected and incubated for 96 h. The parental and reassorted viruses were purified for three rounds and confirmed by sequencing to ensure the

absence of unwanted mutations. Aliquots of viral fluid were stored at -80°C .

Mouse challenge experiments

Six-week-old female BALB/c mice (Yangzhou Experimental Animal Center, Jiangsu, China) were used as animal models to investigate the pathogenicity of these mutated viruses to mammals. Groups of five mice were anaesthetized with Zoletil[®] 50 (tiletamine-zolazepam (Virbac, Carros, France), 20 mg/g body weight) and intranasally (i.n.) inoculated with 50 μL of virus in ten-fold serial dilutions from $10^{3.0}$ to $10^{6.0}$ 50% egg infective dose (EID₅₀). To determine the mouse lethal dose at 50% (MLD₅₀), all mice were monitored daily for 14 days, and death was recorded on a daily basis. Humane euthanasia (overdose CO₂) was used for mice with a body weight loss >25% of their initial body weight. In accordance with Reed and Muench, the MLD₅₀ values were calculated [18]. In each group, three mice were euthanized 3 days post-infection (dpi) and samples from the nasal turbinates, lungs, kidneys, and brain were collected for virus titrations.

The lungs of mice infected with the indicated viruses at 3 dpi were harvested, fixed in 10% neutral-buffered formalin, embedded in paraffin, and sliced into 4 μm sections. Hematoxylin–eosin (H&E) staining was performed on the sections. Lung tissue sections were scored based on pathological changes: 0, no visible lesions; 1, area affected by the lesions (<10%); 2, area affected by the lesions (<30%, \geq 10%); 3, area affected by the lesions (<50%, \geq 30%); and 4, area affected by the lesions (\geq 50%). We measured lung edema based on the ratio of wet to dry weight of the lungs of virus-inoculated or control mice. The lungs were then heated to 65°C in a gravity convection oven for 24 h and weighed to obtain the dry mass. The wet/dry weight ratio was calculated by dividing the dry mass by the wet mass.

Quantitative real-time PCR (qRT-PCR) was used to qualitatively assess the levels of Mx1, interferon-beta (IFN- β), interleukin-beta (IL-1 β), IL-6, inducible protein-10 (IP-10) and interferon-stimulated gene 15 (ISG15) in lung homogenates. In brief, the lung homogenates were collected at 3 dpi, RNA was extracted and converted into cDNA, and then the levels of cytokine expression were analysed with TB Green premix Ex Taq[™] II on a LightCycler 480 System instrument. The expression of glyceraldehyde-3-phosphate dehydrogenase (GAPDH) was also detected and used to normalize gene expression between samples.

Viral replication in different host cell lines

To evaluate growth dynamics *in vitro* in different cell lines, MDCK, A549 and CEF cells were grown on 6-well

plates and infected with the indicated viruses at a multiplicity of infection (MOI) of 0.001 and a 50% tissue culture infectious dose (TCID₅₀). Following 1 h of incubation, the viruses were removed, and the cells were washed three times with PBS. The cells were incubated at 37 °C with essential medium containing 0.5% BSA. At 12, 24, 36, 48, 60 and 72 h post-infection (hpi), virus-containing culture supernatants were harvested. Viral titres are expressed as the TCID₅₀/mL in MDCK cells.

Polymerase activity assay

Viral polymerase activity was determined using a luciferase reporting assay. Viral ribonucleoprotein (vRNP) complexes composed of PB2, PB1, PA and nucleoprotein (NP) derived from JTC4 and JTC11 were separately cloned and inserted into the pCAGGS vector. HEK293T cells were co-transfected with PB2, PB1, PA, and NP expression plasmids (200 ng) together with the firefly luciferase reporter plasmid p-Luci (300 ng) and the internal control Renilla plasmid (30 ng). At 24 h, the cell lysates were processed to measure firefly and Renilla luciferase activities using a GluMax 96 microplate luminometer (Promega).

Statistical analysis

We used GraphPad Prism 9 for graphing and statistical analyses (GraphPad Software, San Diego, CA, USA). To make one-way comparisons between multiple groups, one-way ANOVA was used, and two-way ANOVA was used to make two-way comparisons. Statistical

significance was reported at $P < 0.05$, $*P < 0.05$, $**P < 0.01$, $***P < 0.001$, and $****P < 0.0001$.

Results

Polymerase proteins cooperatively increased H7N9 virulence in mice

The JTC4 and JTC11 viruses differ by only six amino acids located in five different proteins, i.e., PB2, PB1, PA, HA and NA. While the pathogenicity and host-range specificity of AIVs are influenced by multiple genetic factors, the polymerase protein plays a crucial role in determining these properties [19–21]. To identify amino acids in the polymerase protein of JTC11 that contribute to its high virulence in mice, we compared the PB2, PB1 and PA sequences of JTC4 and JTC11. Only three amino acids (PB2-627E/K, PB1-719V/M and PA-444 N/D) were different [16]. According to previous studies, the PB2-E627K substitution is critical for mammalian adaptation [17, 19], and the other two amino acids have not previously been linked to the pathogenicity of influenza viruses. We therefore generated seven reassortants by reverse genetics using JTC4 as the backbone (Figure 1). We designated these reassortants rPB2^{E627K}, rPB1^{V719M}, rPA^{N444D}, rPB2^{E627K}+PB1^{V719M}, rPB2^{E627K}+PA^{N444D}, rPB1^{V719M}+PA^{N444D}, and rPB2^{E627K}+PB1^{V719M}+PA^{N444D} and tested their replication and virulence in mice.

First, we infected mice with viruses with single mutations in the background of JTC4. As shown in Figure 2, all single-point mutation viruses (rPB2^{E627K}, rPB1^{V719M}, and rPA^{N444D}) caused minor weight loss and no deaths

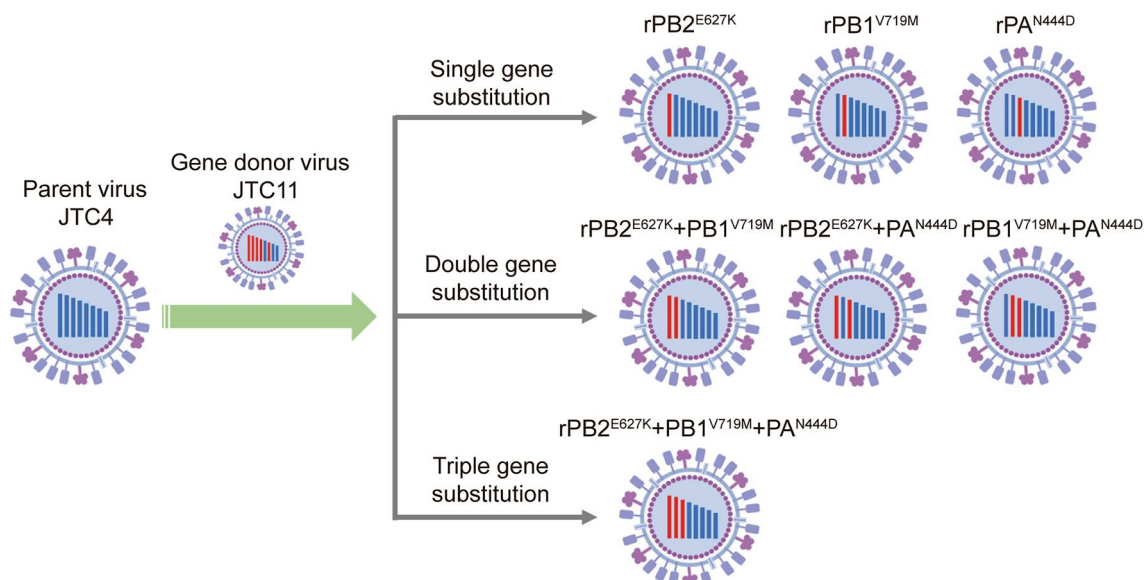


Figure 1 Schematic composition of the gene replacement of H7N9 viruses. The eight gene segments of the virus are, from left to right, polymerase B2 (PB2), polymerase B1 (PB1), polymerase A (PA), hemagglutinin (HA), nucleoprotein (NP), neuraminidase (NA), matrix protein (M), and non-structural protein (NS). Blue represents JTC4, while red indicates the genes differing between JTC11 and JTC4.

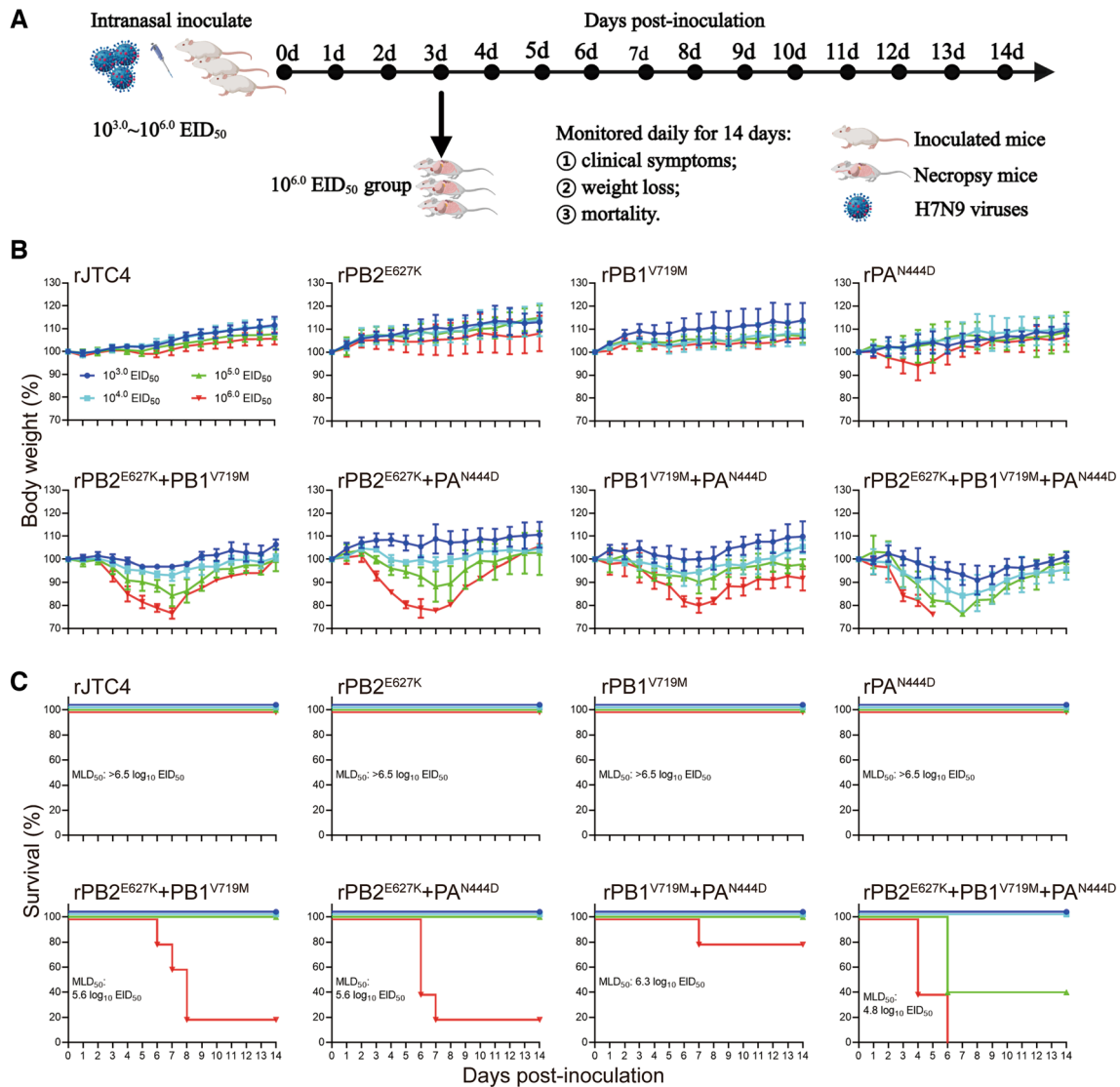


Figure 2 Mapping of crucial mutation sites in polymerase proteins that increase H7N9 AIV virulence in mice. **A** Diagram of the experimental procedure. Briefly, groups of 6-week-old five BALB/c mice were inoculated with the indicated viruses at doses of $10^{3.0} \sim 10^{6.0}$ EID₅₀; clinical symptoms, body weight and survival were monitored daily for 14 dpi; mice were humanely killed when they lost $\geq 25\%$ of their initial body weight; and $10^{6.0}$ EID₅₀ group mice were dissected and sampled on day 3 to detect viral load. **B** Body weight loss was monitored for 14 days. **C** Survival was monitored for 14 days.

under high-dose infection conditions ($10^{6.0}$ EID₅₀), with an MLD₅₀ > 6.5 log₁₀ EID₅₀, indicating that single-point mutations do not affect the pathogenicity of H7N9 in mice. This finding is consistent with the finding that single-point mutation viruses replicate at extremely low titres in multiple organs of mice, even in the lungs (Figure 3). Afterwards, we examined the pathogenicity of the double-point combined mutation strains. As shown in Figure 2, significant weight loss and death were observed in all double-point combined mutation strains (rPB2^{E627K}+PB1^{V719M}, rPB2^{E627K}+PA^{N444D}, and

rPB1^{V719M}+PA^{N444D}) under $10^{6.0}$ EID₅₀ infection conditions, with MLD₅₀ values of 5.6, 5.6 and 6.3 log₁₀ EID₅₀, respectively. In addition, these double-point combined mutation strains could increase replication in all organs of mice, even in the brain (Figure 3). These results showed that all double-point synergistic mutations could enhance H7N9 subtype AIV virulence in mice. Additionally, the combined mutant strains of PB2, PB1 and PA (rPB2^{E627K}+PB1^{V719M}+PA^{N444D}) further enhanced the virulence of H7N9 in mice (Figure 2), increasing its ability to replicate in various organs (Figure 3). Taken

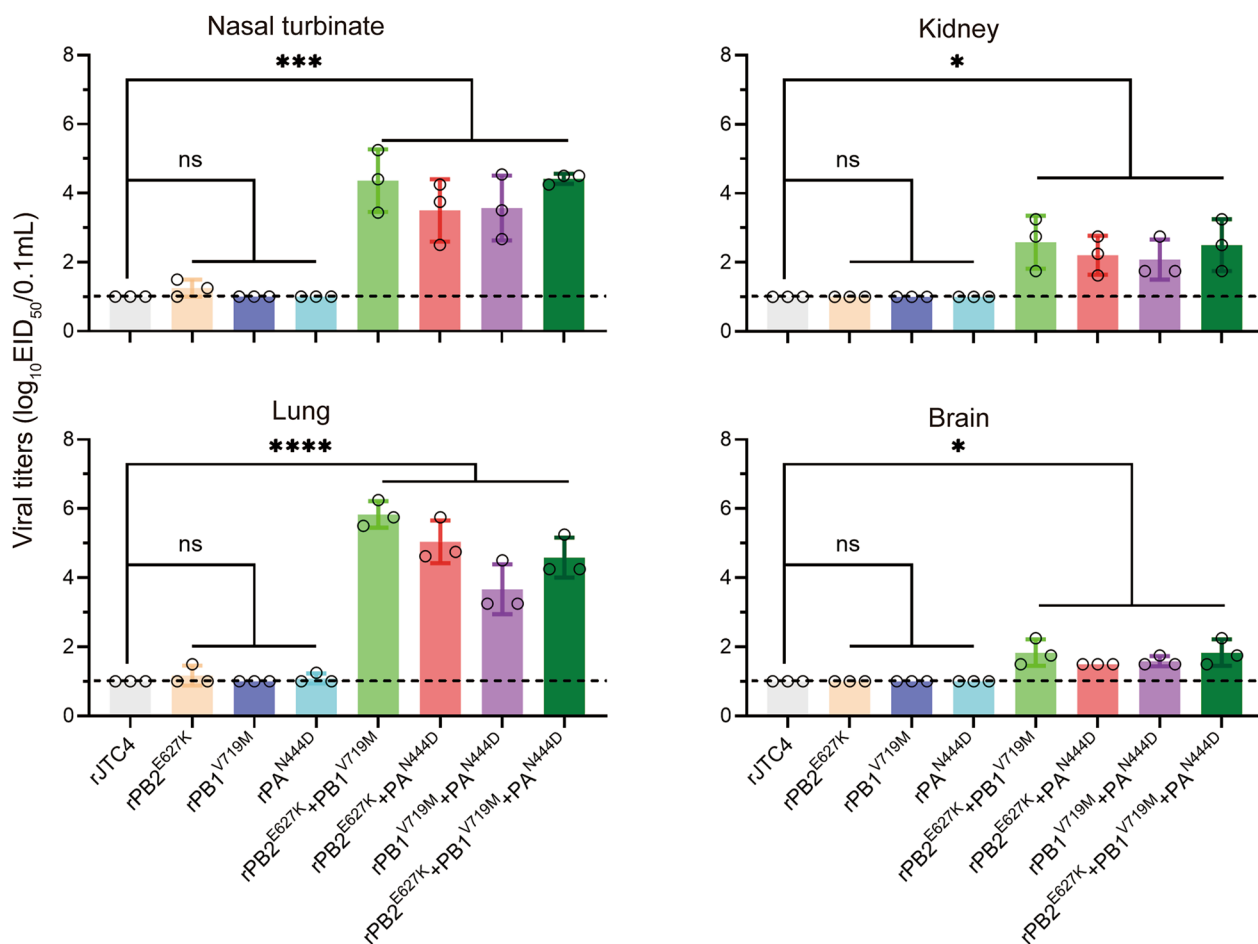


Figure 3 Polymerase proteins cooperatively increased H7N9 replication in mice. Mice were challenged with 10^{6.0} EID₅₀ of the indicated virus, and three mice per group were euthanized at 3 dpi; virus titres in different organs (turbinate, lung, brain, and kidney) were determined by an EID₅₀ assay on chicken eggs; horizontal dashed lines indicate the lower limits of detection.

together, the synergy among polymerase proteins plays a crucial role in the heightened pathogenicity of H7N9 in mammals.

Polymerase proteins cooperatively enhance the ability of H7N9 to induce lung injury and inflammation

AIVs primarily target the lungs of mammals, resulting in life-threatening lung damage and severe inflammation. After infection with the indicated viruses at an EID₅₀ of 10^{6.0}, the mice were euthanized on day 3, and the lungs were studied histopathologically. The double-point and three-point combined mutation strains induced pulmonary lesions and focal dark red consolidations (Figures 4E–H). These features were not detected in the lungs of mice inoculated with the single-point mutation viruses (Figures 4B–D). The lungs of the double-point and three-point mutation strain-infected mice showed severe peribronchiolitis as well as bronchopneumonia (thickened alveolar septa, edema, and interstitial inflammatory cells

infiltrating the alveoli), whereas mild pathological damage was observed in the lungs of the single mutation viruses (Figure 4). The histopathology scores of the double-point and three-point mutation strain-infected lungs reached 2.0, whereas those of the single-point mutation virus-infected lungs were less than 1.0 (Figure 4).

As indicated by the wet-to-dry ratio, the lungs of mice inoculated with the double-point and three-point mutation strains exhibited significant inflammation (Figure 4I). Inflammation is strongly associated with the pathogenicity of AIVs. Afterwards, we evaluated whether mouse lungs were infiltrated with inflammatory cytokines after infection with rJTC4 and single- and multipoint mutation viruses. As shown in Figure 5, the levels of proinflammatory cytokines (IL-1β and IL-6), chemokines (IP-10), and antiviral cytokines (IFN-β, Mx1, and ISG15) were notably elevated in the groups inoculated with multipoint mutation viruses compared to those inoculated with rJTC4. Taken together, these

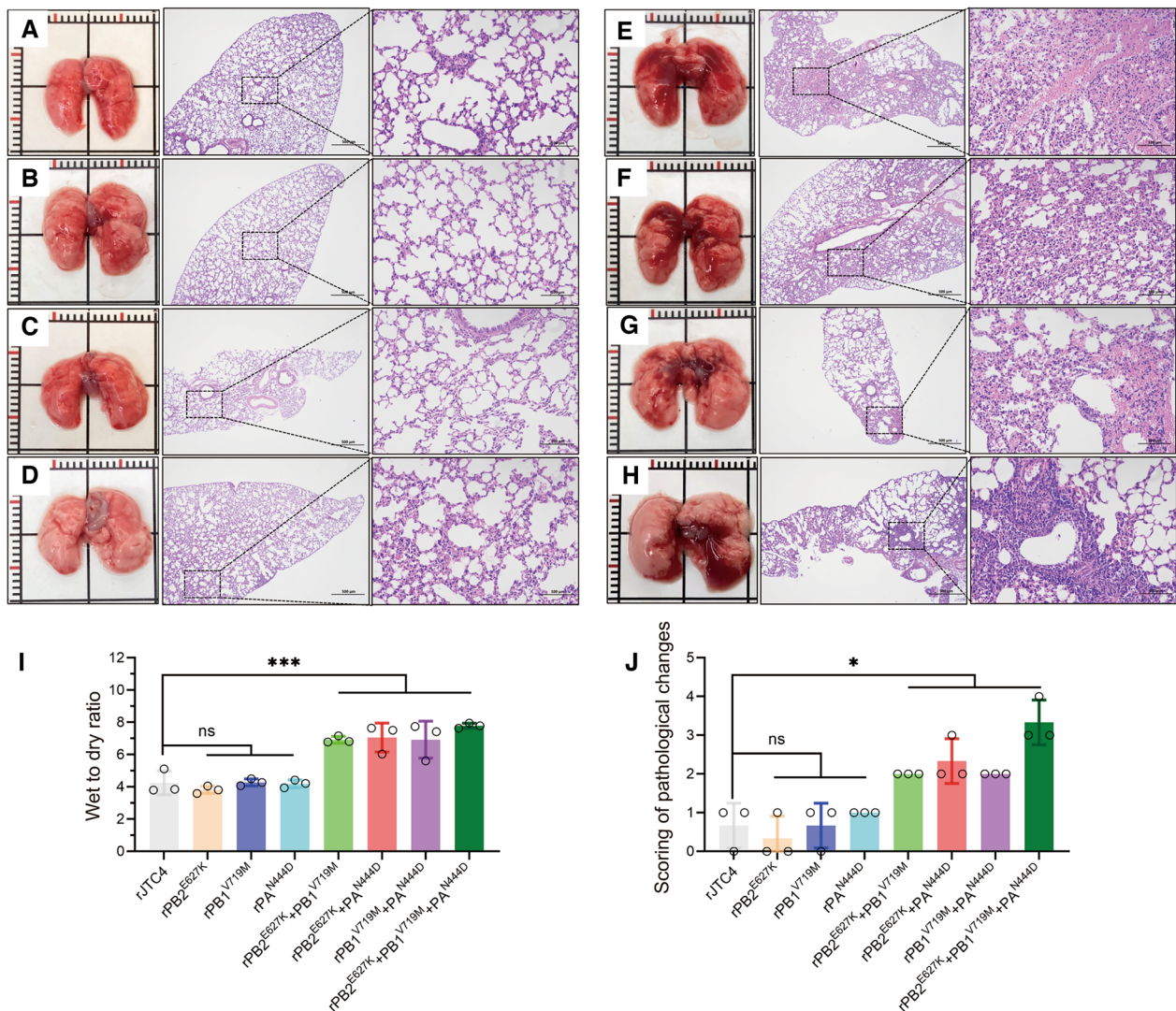


Figure 4 Polymerase proteins cooperatively increased H7N9-induced lung lesions in mice. Macroscopic lesions and histopathological (lung sections were stained with H&E) findings in the lungs of mice infected with the indicated viruses at an EID₅₀ of 10^{6.0} at 3 dpi. **A–H** rJTC4, rPB2^{E627K}, rPB1^{V719M}, rPA^{N444D}, rPB2^{E627K} + rPB1^{V719M}, rPB2^{E627K} + rPA^{N444D}, rPB1^{V719M} + rPA^{N444D}, and rPB2^{E627K} + rPB1^{V719M} + rPA^{N444D}, respectively. **I** Lung edema was assessed using the lung wet/dry weight ratio. Briefly, the lungs of each virus-inoculated or control mouse were collected and weighed to obtain the wet mass. The lungs were then heated to 65 °C in a gravity convection oven for 24 h and weighed to obtain the dry mass. The wet/dry weight ratio was calculated by dividing the dry mass by the wet mass. **J** Histopathological scores of the lungs of mice inoculated with the indicated viruses. Lung tissue sections were scored based on pathological changes: 0, no visible lesions; 1, area affected by the lesions (<10%); 2, area affected by the lesions (<30%, ≥10%); 3, area affected by the lesions (<50%, ≥30%); and 4, area affected by the lesions (≥50%).

results indicate that polymerase proteins cooperatively enhance the ability of H7N9 to induce lung injury and inflammation.

Polymerase proteins cooperatively enhance the ability of H7N9 to replicate in mammalian cells

The replication ability of multipoint mutation viruses was tested in different host cells to mimic host-switching events in vitro. To quantify viral replication dynamics during overt infection (0–72 hpi), MDCK, A549 and

CEF cells were inoculated with the indicated viruses at an MOI of 0.001. As shown in Figure 6, multipoint mutation viruses generated significantly higher titres than did the rJTC4 virus during the initial infection stages to late infection stages in mammalian cells (MDCK, A549). Additionally, multipoint mutation viruses lose their ability to replicate in CEFs. According to these results, multipoint mutations in polymerase proteins increase viral replication in mammalian cells and decrease viral replication in CEFs.

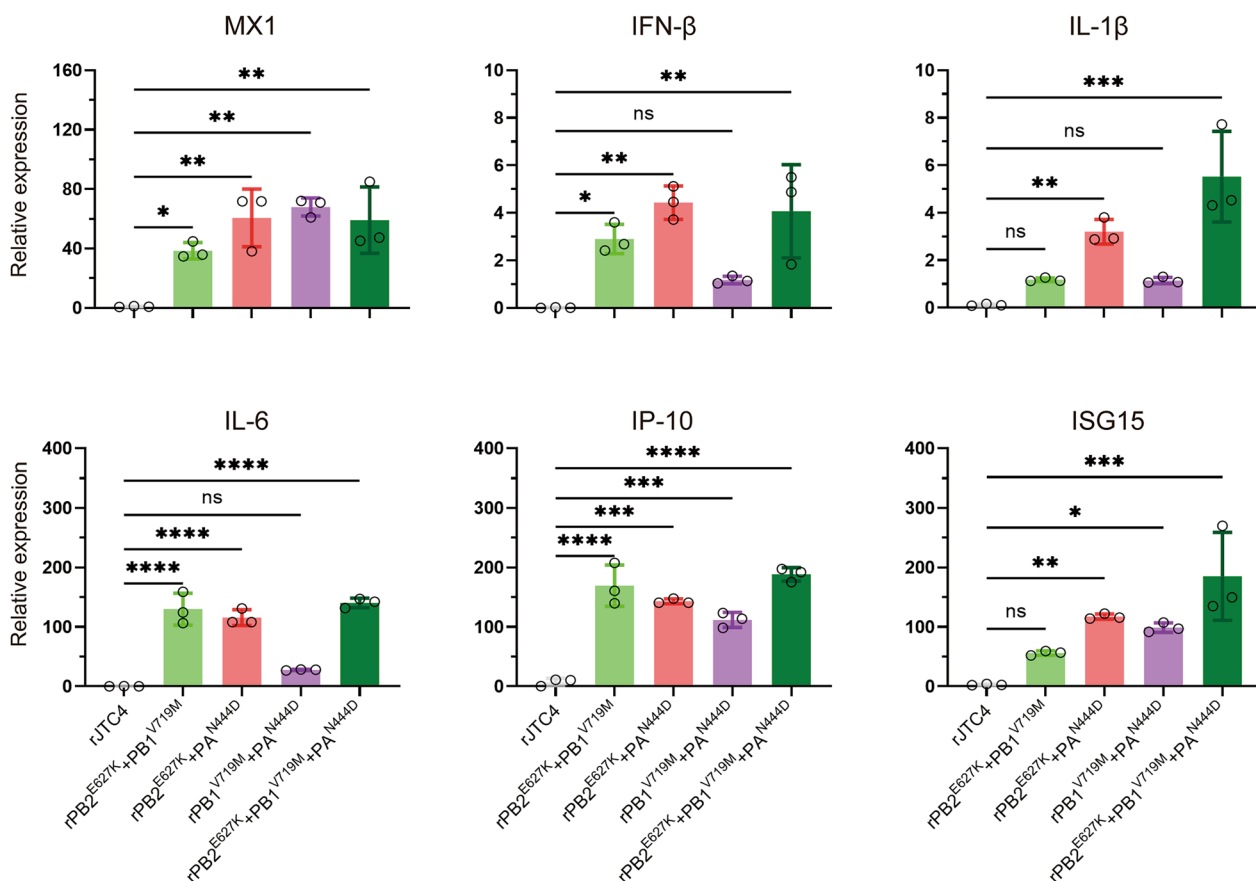


Figure 5 Inflammatory cytokine expression of the reassortant H7N9 isolates in mice. Mice were inoculated intranasally with $10^{6.0}$ EID₅₀ of the desired viruses, total RNA was extracted from the lungs at 3 dpi, and equal amounts of RNA were used for qRT-PCR. The expression level of each cytokine gene was normalized to that of GAPDH and is presented as the fold change compared with the control.

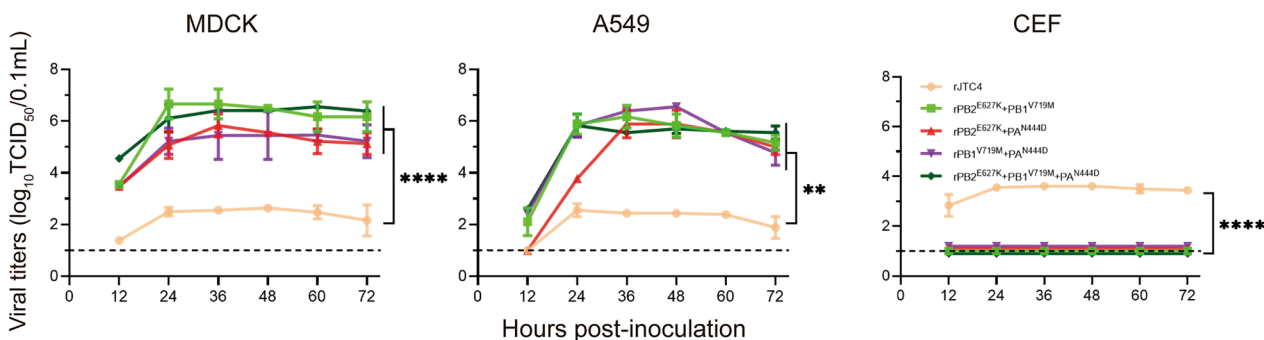


Figure 6 Growth dynamics of the reassortant H7N9 viruses in different cell lines. MDCK, A549, and CEF cells were inoculated with the indicated viruses at a multiplicity of infection (MOI) of 0.001 TCID₅₀/cell in triplicate at 37 °C. The supernatants were aseptically harvested at 12, 24, 36, 48, 60 and 72 hpi. The virus titres were determined by determining the TCID₅₀ per 0.1 mL in MDCK cells.

Polymerase proteins cooperatively enhance the polymerase activity of H7N9 in mammalian cells

There is evidence that the viral RNP complex plays a key role in the replication and pathogenicity of AIVs [22, 23]. To ascertain the relative contribution of mutations

to RNP polymerase activity, minigenome replication assays were conducted in HEK293T cells at 33 °C and 37 °C (corresponding to the temperatures of the human upper and lower respiratory tracts, respectively [24]). The polymerase activities of rPB2^{E627K}, rPB2^{E627K} + PB1^{V719M},

rPB2^{E627K} + PA^{N444D} and rPB2^{E627K} + PB1^{V719M} + PA^{N444D} were significantly greater than those of rJTC4 at 33 °C and 37 °C (Figure 7). In addition, the polymerase activity of rPB1^{V719M} + PA^{N444D} was significantly greater than that of rJTC4 at 37 °C but not at 33 °C (Figure 7). These findings suggest that the polymerase activities of H7N9, which possesses PB2-627K alone or PB2-627K combined with PB1-719M and PA-444D, are greater than those of rJTC4 in mammalian cell lines.

Prevalence of amino acid types at positions PB2-627, PB1-719 and PA-444 in H7N9 viruses

To determine the prevalence of the amino acids PB2-627, PB1-719 and PA-444 in different host-derived H7N9 viruses, available H7N9 PB2, PB1 and PA sequences were downloaded from the Global Initiative on Sharing All Influenza Data (GISAID) and National Center for Biotechnology Information (NCBI) databases [25, 26]. As of December 2023, H7N9 was the subtype with the highest number (1568) of human AIV infection cases. Among these PB2 segments originating from humans, 71.02% carry the E627K mutation (Table 1). In contrast, only 0.9% of PB2 segments originating from avians exhibited the E627K mutation. As shown in Table 1, PB1-719V (99.74%) and 719M (0.13%) were detected in avian-derived H7N9 strains. In addition, there was a slight increase (0.38%) in the proportion of PB1-719M mutations in human-derived H7N9 strains. Similar to PB1-719, PA-444D was also present in natural avian- and

Table 1 Prevalence of amino acid types at positions PB2-627, PB1-719 and PA-444 in H7N9 viruses

Segment	Site	Amino acid substitutions	Relative frequency (no. of strains with the substitution/total no. of strains)	
			Avian-origin	Human-origin
PB2	627	E	98.77% (882/893)	26.35% (331/1256)
		K	0.9% (8/893)	71.02 (892/1256)
		Others	0.33% (3/893)	2.63% (33/1256)
PB1	719	V	99.74% (754/756)	93.7% (1234/1317)
		M	0.13% (1/756)	0.38% (5/1317)
		Others	0.13% (1/756)	5.92% (78/1317)
PA	444	N	99.74% (755/757)	99.46% (1290/1297)
		D	0.26% (2/757)	0.39% (5/1297)
		Others	0 (0/757)	0.15% (2/1297)

human-derived H7N9 strains, and the proportions (0.26% and 0.39%, respectively) were extremely low.

Discussion

In this study, we explored the genetic basis for the difference in virulence between two avian H7N9 viruses in mice. The JTC11 virus was lethal in mice, with an MLD₅₀ of 3.5 log₁₀ EID₅₀, whereas the JTC4 virus was nonlethal in mice, with an MLD₅₀ of >6.5 log₁₀ EID₅₀ [16]. Using a reverse genetic system, we found that polymerase proteins are key to H7N9 virulence in mice.

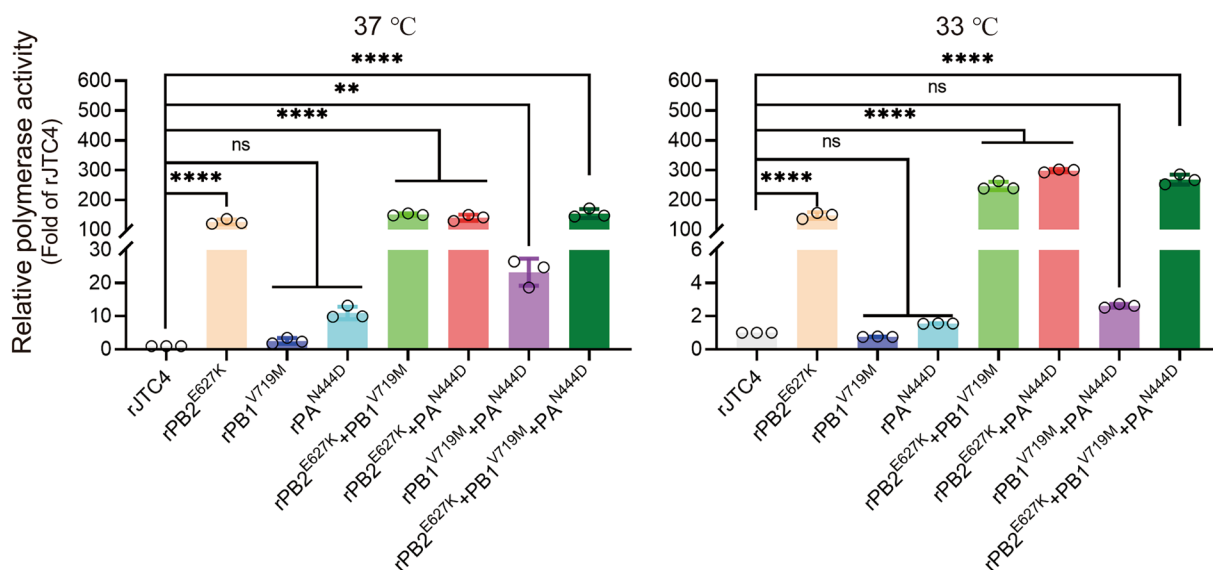


Figure 7 Polymerase proteins cooperatively increase H7N9 polymerase activity in mammalian cells. Plasmids encoding the PB2, PB1, PA, and NP proteins derived from JTC4 with the indicated segment substitutions were transfected into HEK293T cells at the indicated temperatures, together with the firefly luciferase reporter plasmid and internal control plasmid. At 24 h post-transfection, luciferase activities were measured.

vRNPs contain the viral RNA genome complexed with multiple NP molecules and one RNA-dependent RNA polymerase complex containing PB2, PB1, and PA [27]. The results of homology modelling (Additional file 1) indicated that the PB1-V719M mutation alters the interaction between PB1 and PB2, while the PA-N444D mutation affects the interaction between PA and PB1. These structural changes in the vRNP complex suggest potential alterations in protein function. These vRNPs are the minimal units required for viral transcription and replication [27]. Host restriction factors can block vRNP function, and mammalian AIVs are particularly susceptible to this [28–31]. Therefore, polymerases exhibit limited efficiency in replicating the genome within mammalian cells. AIVs can propagate between mammals, and a high mutation rate in the genome is an important strategy [19, 32–35]. Several host-adaptive mutations in viral polymerase subunits have been identified [20, 21, 23, 36, 37]. The most commonly known adaptive mutation is PB2-E627K: human-adapted AIVs typically encode K, whereas avian AIVs encode E [38, 39]. Notably, several studies have shown that PB2-627K alone can overcome species restriction and increase AIV virulence in mammals [38, 40, 41]. However, in the present study, the PB2-E627K mutation alone was insufficient to increase H7N9 virulence in mice despite its ability to increase polymerase activity in mammalian cells at both 33 °C and 37 °C.

In most cases, host adaptation and pathogenicity of AIVs in mammals are polygenic traits [17, 22, 42, 43]. As we previously reported, we found that hemagglutinin mutations combined with PB2-627K can enhance the pathogenicity and transmissibility of avian H9N2 in mammals [17]. Liang et al. discovered that the emergence of the PB2-E627K mutation in H7N9 AIVs is driven by the intrinsically low polymerase activity associated with the PA protein. This highlights the crucial role of cooperation among polymerase proteins in facilitating AIV adaptation within mammalian hosts [22]. Our results showed that $rPB2^{E627K} + PB1^{V719M}$, $rPB2^{E627K} + PA^{N444D}$, and $rPB2^{E627K} + PB1^{V719M} + PA^{N444D}$ can increase the virulence of H7N9 in mice. Consistent with this, PB1-V719M and/or PA-N444D mutation combined with PB2-E627K further increased polymerase activity in mammalian cells at both 33 °C and 37 °C.

The PB2-E627K mutation first appeared in the 1918 H1N1 pandemic virus, and all human circulating viruses of the twentieth century possessed this signature [44]. H7N9, with 1568 reported human infection cases, stands out as the subtype with the highest incidence. Notably, 71.02% of human-derived viruses harbor the PB2-E627K mutation, underscoring the significance of PB2-627K in AIV adaptation to mammals. In this study, the PB1-V719M and/or PA-N444D mutation combined with

PB2-E627K increased virulence in mice. However, the PB1-719M and PA-444D mutations were not prevalent in the current H7N9 strains.

In summary, our findings demonstrate that the cooperation of PB2-E627K, PB1-V719M, and PA-N444D potentially contributes to enhancing the virulence of avian H7N9 in mice. Additionally, we observed that these combined mutations augment polymerase activity, thereby enhancing virus replication, inflammatory cytokine expression, and lung injury, ultimately increasing pathogenicity in mice. Moreover, our study emphasized that AIV virulence is a polygenic trait. The identification of these newly associated virulence-related residues in vRNPs may serve as an early warning for future human pandemics.

Supplementary Information

The online version contains supplementary material available at <https://doi.org/10.1186/s13567-024-01342-6>.

Additional file 1 Effects of mutation on the three-dimensional structure of polymerase proteins.

Acknowledgements

The authors would like to acknowledge Zhuxing Ji (College of Veterinary Medicine, Yangzhou University, Yangzhou, 225009, China) for critical revision of the manuscript.

Authors' contributions

XW and KL conceived of and designed the project. XW, HZ, XT, RG and KL performed the experiments. XW, XT, XL (Xiaolong Lu), WY, YC, LZ, JH, SH, MG, and XL (Xiaowen Liu) participated in the data acquisition and analysis. XW and XT wrote the original draft of the manuscript. XL (Xiufan Liu) and KL helped with manuscript review and editing. XL (Xiufan Liu) and KL supervised the project. All the authors have read and approved the final manuscript.

Funding

This work was supported by the National Key Research and Development Project of China (2021YFD1800202); the National Natural Science Foundation of China (32302958); the Youth Program of the Natural Science Foundation of Jiangsu Province (BK20230575, BK20220580); the Natural Science Foundation of the Jiangsu Higher Education Institutions of China (22KJJD230002); the Ear-marked Fund for China Agriculture Research System (CARS-40); the 111 Project D18007; and the Priority Academic Program Development of Jiangsu Higher Education Institutions (PAPD).

Availability of data and materials

The data supporting the conclusions of this article are included within the article. Additional data used and/or analysed during the current study are available from the corresponding author upon reasonable request.

Declarations

Ethics approval and consent to participate

The study was conducted in strict adherence to the guidelines outlined in the Guide for the Care and Use of Laboratory Animals by the Ministry of Science and Technology of the People's Republic of China. All experiments involving live virulent H7N9 viruses and animals were carried out in animal biosafety level 3 (ABSL-3) facilities at Yangzhou University in accordance with the recommendations specified in the institutional biosafety manual. The Committee for Laboratory Animals (Permission number: SYXK-SU-2022-0044) and the Institutional Biosafety Committee of Yangzhou University approved all experiments, ensuring compliance with the guidelines set forth by the Jiangsu Laboratory

Animal Welfare and Ethics Committee of the Jiangsu Administrative Committee of Laboratory Animals.

Competing interests

The authors declare that they have no competing interests.

Received: 21 March 2024 Accepted: 14 June 2024

Published online: 05 July 2024

References

- Wu Y, Wu Y, Tefsen B, Shi Y, Gao GF (2014) Bat-derived influenza-like viruses H17N10 and H18N11. *Trends Microbiol* 22:183–191
- Tong S, Li Y, Rivaller P, Conrardy C, Castillo DA, Chen LM, Recuenco S, Ellison JA, Davis CT, York IA, Turmelle AS, Moran D, Rogers S, Shi M, Tao Y, Weil MR, Tang K, Rowe LA, Sammons S, Xu X, Frace M, Lindblade KA, Cox NJ, Anderson LJ, Rupprecht CE, Donis RO (2012) A distinct lineage of influenza A virus from bats. *Proc Natl Acad Sci USA* 109:4269–4274
- Long JS, Mistry B, Haslam SM, Barclay WS (2019) Host and viral determinants of influenza A virus species specificity. *Nat Rev Microbiol* 17:67–81
- Liu M, van Kuppeveld FJ, de Haan CA, de Vries E (2023) Gradual adaptation of animal influenza A viruses to human-type sialic acid receptors. *Curr Opin Virol* 60:101314
- Wang D, Zhu W, Yang L, Shu Y, *Epidemiology T* (2021) Virology, and pathogenicity of human infections with avian influenza viruses. *Cold Spring Harb Perspect Med* 11:a038620
- Shen YY, Ke CW, Li Q, Yuan RY, Xiang D, Jia WX, Yu YD, Liu L, Huang C, Qi WB, Sikkema R, Wu J, Koopmans M, Liao M (2016) Novel reassortant avian influenza A(H5N6) viruses in humans, Guangdong, China, 2015. *Emerg Infect Dis* 22:1507–1509
- Li KS, Guan Y, Wang J, Smith GJ, Xu KM, Duan L, Rahardjo AP, Puthavathana P, Buranathai C, Nguyen TD, Estoepongastie AT, Chaisingh A, Auewarakul P, Long HT, Hanh NT, Webby RJ, Poon LL, Chen H, Shortridge KF, Yuen KY, Webster RG, Peiris JS (2004) Genesis of a highly pathogenic and potentially pandemic H5N1 influenza virus in eastern Asia. *Nature* 430:209–213
- Tong XC, Weng SS, Xue F, Wu X, Xu TM, Zhang WH (2018) First human infection by a novel avian influenza A(H7N4) virus. *J Infect* 77:249–257
- Chen Y, Liang W, Yang S, Wu N, Gao H, Sheng J, Yao H, Wo J, Fang Q, Cui D, Li Y, Yao X, Zhang Y, Wu H, Zheng S, Diao H, Xia S, Zhang Y, Chan KH, Tsoi HW, Teng JL, Song W, Wang P, Lau SY, Zheng M, Chan JF, To KK, Chen H, Li L, Yuen KY (2013) Human infections with the emerging avian influenza A H7N9 virus from wet market poultry: clinical analysis and characterisation of viral genome. *Lancet* 381:1916–1925
- Chen H, Yuan H, Gao R, Zhang J, Wang D, Xiong Y, Fan G, Yang F, Li X, Zhou J, Zou S, Yang L, Chen T, Dong L, Bo H, Zhao X, Zhang Y, Lan Y, Bai T, Dong J, Li Q, Wang S, Zhang Y, Li H, Gong T, Shi Y, Ni X, Li J, Zhou J, Fan J, Wu J, Zhou X, Hu M, Wan J, Yang W, Li D, Wu G, Feng Z, Gao GF, Wang Y, Jin Q, Liu M, Shu Y (2014) Clinical and epidemiological characteristics of a fatal case of avian influenza A H10N8 virus infection: a descriptive study. *Lancet* 383:714–721
- Qi X, Qiu H, Hao S, Zhu F, Huang Y, Xu K, Yu H, Wang D, Zhou L, Dai Q, Zhou Y, Wang S, Huang H, Yu S, Huo X, Chen K, Liu J, Hu J, Wu M, Bao C (2022) Human infection with an avian-origin influenza A (H10N3) virus. *N Engl J Med* 386:1087–1088
- Yang R, Sun H, Gao F, Luo K, Huang Z, Tong Q, Song H, Han Q, Liu J, Lan Y, Qi J, Li H, Chen S, Xu M, Qiu J, Zeng G, Zhang X, Huang C, Pei R, Zhan Z, Ye B, Guo Y, Zhou Y, Ye W, Yao D, Ren M, Li B, Yang J, Wang Y, Pu J, Sun Y, Shi Y, Liu WJ, Ou X, Gao GF, Gao L, Liu J (2022) Human infection of avian influenza A H3N8 virus and the viral origins: a descriptive study. *Lancet Microbe* 3:e824–e834
- Xu J, Li S, Yang Y, Liu B, Yang H, Li T, Zhang L, Li W, Luo X, Zhang L, Pan M (2018) Human infection with a further evolved avian H9N2 influenza A virus in Sichuan, China. *Sci China Life Sci* 61:604–606
- Human infection with avian influenza A viruses <https://www.who.int>. 27 Apr 2024.
- Liu K, Ding P, Pei Y, Gao R, Han W, Zheng H, Ji Z, Cai M, Gu J, Li X, Gu M, Hu J, Liu X, Hu S, Zhang P, Wang X, Wang X, Liu X (2022) Emergence of a novel reassortant avian influenza virus (H10N3) in Eastern China with high pathogenicity and respiratory droplet transmissibility to mammals. *Sci China Life Sci* 65:1024–1035
- Wang X, Zheng H, Gao R, Ren L, Jin M, Ji Z, Wang X, Lu X, Yang W, Gu M, Liu X, Hu S, Liu K, Liu X (2023) Genetically related avian influenza H7N9 viruses exhibit different pathogenicity in mice. *Animals (Basel)* 13:3680
- Liu K, Guo Y, Zheng H, Ji Z, Cai M, Gao R, Zhang P, Liu X, Xu X, Wang X, Liu X (2023) Enhanced pathogenicity and transmissibility of H9N2 avian influenza virus in mammals by hemagglutinin mutations combined with PB2-627K. *Virol Sin* 38:47–55
- Reed LJ, Muench H (1938) A simple method of estimating fifty per cent endpoints. *Am J Epidemiol* 27:493–497
- Liu WJ, Li J, Zou R, Pan J, Jin T, Li L, Liu P, Zhao Y, Yu X, Wang H, Liu G, Jiang H, Bi Y, Liu L, Yuen KY, Liu Y, Gao GF (2020) Dynamic PB2-E627K substitution of influenza H7N9 virus indicates the in vivo genetic tuning and rapid host adaptation. *Proc Natl Acad Sci USA* 117:23807–23814
- Zhang X, Li Y, Jin S, Zhang Y, Sun L, Hu X, Zhao M, Li F, Wang T, Sun W, Feng N, Wang H, He H, Zhao Y, Yang S, Xia X, Gao Y (2021) PB1 S524G mutation of wild bird-origin H3N8 influenza A virus enhances virulence and fitness for transmission in mammals. *Emerg Microbes Infect* 10:1038–1051
- Mok CK, Lee HH, Lestra M, Nicholls JM, Chan MC, Sia SF, Zhu H, Poon LL, Guan Y, Peiris JS (2014) Amino acid substitutions in polymerase basic protein 2 gene contribute to the pathogenicity of the novel A/H7N9 influenza virus in mammalian hosts. *J Virol* 88:3568–3576
- Liang L, Jiang L, Li J, Zhao Q, Wang J, He X, Huang S, Wang Q, Zhao Y, Wang G, Sun N, Deng G, Shi J, Tian G, Zeng X, Jiang Y, Liu L, Liu J, Chen P, Bu Z, Kawaoaka Y, Chen H, Li C (2019) Low polymerase activity attributed to PA drives the acquisition of the PB2 E627K mutation of H7N9 avian influenza virus in mammals. *MBio* 10:e01162-19
- Xu G, Zhang X, Gao W, Wang C, Wang J, Sun H, Sun Y, Guo L, Zhang R, Chang KC, Liu J, Pu J (2016) Prevailing PA mutation K356R in avian influenza H9N2 virus increases mammalian replication and pathogenicity. *J Virol* 90:8105–8114
- Eccles R (2020) Why is temperature sensitivity important for the success of common respiratory viruses? *Rev Med Virol* 31:1–8
- Global Initiative on Sharing all Influenza Data. <https://platform.gisaid.org>.
- National Center for Biotechnology Information. <https://www.ncbi.nlm.nih.gov>.
- Wandzik JM, Kouba T, Karuppasamy M, Pflug A, Drncova P, Provaznik J, Azevedo N, Cusack S (2020) A structure-based model for the complete transcription cycle of influenza polymerase. *Cell* 4:877–893
- Long JS, Giotis ES, Moncorge O, Frise R, Mistry B, James J, Morisson M, Iqbal M, Vignal A, Skinner MA, Barclay WS (2016) Species difference in ANP32A underlies influenza A virus polymerase host restriction. *Nature* 529:101–104
- Bortz E, Westera L, Maamary J, Steel J, Albrecht RA, Manicassamy B, Chase G, Martinez-Sobrido L, Schwemmler M, Garcia-Sastre A (2011) Host- and strain-specific regulation of influenza virus polymerase activity by interacting cellular proteins. *MBio* 2:e00151-11
- Hudjetz B, Gabriel G (2012) Human-like PB2 627K influenza virus polymerase activity is regulated by importin- α 1 and - α 7. *PLoS Pathog* 8:e1002488
- Resa-Infante P, Bonet J, Thiele S, Alawi M, Stanelle-Bertram S, Tuku B, Beck S, Oliva B, Gabriel G (2019) Alternative interaction sites in the influenza A virus nucleoprotein mediate viral escape from the importin- α 7 mediated nuclear import pathway. *FEBS J* 286:3374–3388
- Zhou Y, Wu X, Yan D, Chen C, Liu X, Huang C, Fu X, Tian G, Ding C, Wu J, Xu J, Li L, Yang S (2021) V292I mutation in PB2 polymerase induces increased effects of E627K on influenza H7N9 virus replication in cells. *Virus Res* 291:198186
- Zhu W, Feng Z, Chen Y, Yang L, Liu J, Li X, Liu S, Zhou L, Wei H, Gao R, Wang D, Shu Y (2019) Mammalian-adaptive mutation NP-Q357K in Eurasian H1N1 Swine Influenza viruses determines the virulence phenotype in mice. *Emerg Microbes Infect* 8:989–999
- Kong H, Ma S, Wang J, Gu C, Wang Z, Shi J, Deng G, Guan Y, Chen H (2019) Identification of key amino acids in the PB2 and M1 proteins of H7N9 influenza virus that affect its transmission in Guinea pigs. *J Virol* 94:e01180-19
- Ma S, Zhang B, Shi J, Yin X, Wang G, Cui P, Liu L, Deng G, Jiang Y, Li C, Chen H (2020) Amino acid mutations A286V and T437M in the nucleoprotein attenuate H7N9 viruses in mice. *J Virol* 94:e01530-19

36. Yamayoshi S, Yamada S, Fukuyama S, Murakami S, Zhao D, Uraki R, Watanabe T, Tomita Y, Macken C, Neumann G, Kawaoka Y (2014) Virulence-affecting amino acid changes in the PA protein of H7N9 influenza A viruses. *J Virol* 88:3127–3134
37. Zhang J, Su R, Jian X, An H, Jiang R, Mok CKP (2018) The D253N mutation in the polymerase basic 2 gene in avian influenza (H9N2) virus contributes to the pathogenesis of the virus in mammalian hosts. *Viol Sin* 33:531–537
38. Subbarao EK, London W, Murphy BR (1993) A single amino acid in the PB2 gene of influenza A virus is a determinant of host range. *J Virol* 67:1761–1764
39. Nilsson BE, Te Velthuis AJW, Fodor E (2017) Role of the PB2 627 domain in influenza A virus polymerase function. *J Virol* 91:e02467-16
40. Hatta M, Gao P, Halfmann P, Kawaoka Y (2001) Molecular basis for high virulence of Hong Kong H5N1 influenza A viruses. *Science* 293:1840–1842
41. Salomon R, Franks J, Govorkova EA, Ilyushina NA, Yen HL, Hulse-Post DJ, Humberd J, Trichet M, Rehg JE, Webby RJ, Webster RG, Hoffmann E (2006) The polymerase complex genes contribute to the high virulence of the human H5N1 influenza virus isolate A/Vietnam/1203/04. *J Exp Med* 203:689–697
42. Dreier C, Resa-Infante P, Thiele S, Stanelle-Bertram S, Walendy-Gnirss K, Speiseder T, Preuss A, Muller Z, Klenk HD, Stech J, Gabriel G (2019) Mutations in the H7 HA and PB1 genes of avian influenza A viruses increase viral pathogenicity and contact transmission in guinea pigs. *Emerg Microbes Infect* 8:1324–1336
43. Yu Z, Ren Z, Zhao Y, Cheng K, Sun W, Zhang X, Wu J, He H, Xia X, Gao Y (2019) PB2 and hemagglutinin mutations confer a virulent phenotype on an H1N2 avian influenza virus in mice. *Arch Virol* 164:2023–2029
44. Taubenberger JK, Reid AH, Lourens RM, Wang R, Jin G, Fanning TG (2005) Characterization of the 1918 influenza virus polymerase genes. *Nature* 437:889–893

Publisher's Note

Springer Nature remains neutral with regard to jurisdictional claims in published maps and institutional affiliations.